

---

# Policy Learning based on Deep Koopman Representation

---

Wenjian Hao<sup>1\*</sup> Paulo C. Heredia<sup>1</sup> Bowen Huang<sup>2</sup> Zehui Lu<sup>1</sup> Zihao Liang<sup>1</sup>  
 Shaoshuai Mou<sup>1†</sup>

<sup>1</sup>Purdue University <sup>2</sup>Pacific Northwest National Laboratory  
 {hao93, pheredia, lu846, liang331, mous}@purdue.edu  
 {bowen.h}@pnnl.gov

## Abstract

This paper proposes a policy learning algorithm based on the Koopman operator theory and policy gradient approach, which seeks to approximate an unknown dynamical system and search for optimal policy simultaneously, using the observations gathered through interaction with the environment. The proposed algorithm has two innovations: first, it introduces the so-called deep Koopman representation into the policy gradient to achieve a linear approximation of the unknown dynamical system, all with the purpose of improving data efficiency; second, the accumulated errors for long-term tasks induced by approximating system dynamics are avoided by applying Bellman's principle of optimality. Furthermore, a theoretical analysis is provided to prove the asymptotic convergence of the proposed algorithm and characterize the corresponding sampling complexity. These conclusions are also supported by simulations on several challenging benchmark environments.

## 1 Introduction

Reinforcement learning (RL) is a type of machine learning algorithm that focuses on training agents to make decisions in an environment by maximizing a reward function over time. In RL, the agent interacts with the environment and receives feedback in the form of rewards for its actions. Recently, RL has gained increasing attention due to its potential for solving complex problems in various domains, including natural language processing [1–5], robotics [6–11], and game playing [12–15].

RL approaches are distinguished into two main categories, model-free and model-based methods. Unlike the traditional model-based control techniques, which typically require a good understanding of the system (e.g., the mathematical dynamics model), model-free RL (MFRL) seeks to approximate the so-called action-value function [16] and directly parameterize the control policy. Then the (near) optimal policy is found by tuning the policy's parameters to minimize the resulting action-value function based on the (stochastic) gradient descent approach, which is also referred to as the policy gradient (PG) method [17]. These methods enable MFRL to deal with complex tasks in complex environments without knowledge of dynamics. Along this direction, some popular work, for instance, "Deep Q Network (DQN)" [18], "Proximal Policy Optimization" [19], and "Actor-critic (AC)" [20] are proposed to solve tasks with discrete action spaces, and in [21] the author proposed an actor-critic approach based on the deterministic policy gradient (DPG) algorithm [22] to extend DQN method to continuous action space scenarios. Nevertheless, MFRL methods typically require plenty of trials to find the optimal policy for given tasks. In particular, recent work [23] provided the theoretical analysis for both on-policy and off-policy DPG algorithms, yielding a result on the sample complexity

---

\*W. Hao is a PhD student at Purdue University

†S. Mou is an associate professor at Purdue University

$\mathcal{O}(\epsilon^{-2})$  for achieving the stationary policy with  $\epsilon$  accuracy, which may be data-inefficient for some robotic systems with limited computational capability.

On the contrary, model-based RL (MBRL) involves learning a model to describe how an agent interacts with the environment. This model includes information about the dynamics of the environment, such as how the environment will change in response to the agent’s actions. The agent then uses this model to generate its actions in order to maximize its cumulative reward. When compared with MFRL, MBRL generally requires less data due to its understanding of environmental dynamics. However, MBRL may necessitate greater computational resources and could be less resilient to inaccuracies in its model [24]. Typically, MBRL can be achieved through two methods: either by possessing prior knowledge of the environment or by using deep neural networks (DNNs) to model the environment based on observed data. The former can be challenging, particularly for high-dimensional systems, as it requires a considerable amount of expertise and knowledge of the dynamics. The latter may require significant computational resources because the unknown environmental dynamics might be extremely nonlinear and complicated. In contrast, MFRL requires the agent to invest a significant amount of effort in exploration and interaction without prior knowledge of the environment. Therefore, acknowledging the aforementioned drawbacks of current MFRL methods and further releasing the requirement of prior knowledge of the environment, this paper proposes a data-efficient MBRL method that does not require prior knowledge of the environment. In addition, the proposed method provides a convergence analysis that guarantees convergence.

**Claim of contributions.** This paper proposes an MBRL framework, named *policy gradient with deep Koopman representation* (PGDK), which consists of three modules with the intention of approximating the *system dynamics* and *value function*, and searching the optimal *policy* simultaneously, and based on the observations while interacting with the environment. The proposed method, which employs the deep Koopman representation (DKR) to approximate system dynamics, is capable of representing complex nonlinear models in a linear form with reasonable error bound [25]. This is in contrast to existing methods that use DNNs for the approximation of system dynamics. As a result, the proposed method enables a more effective control design for complex systems. The proposed method also has superior data efficiency and faster convergence rates when compared with the existing MFRL methods. The other benefit of our algorithm is the prevention of accumulated prediction errors through the utilization of an estimated value function that relies on Bellman’s principle of optimality. Finally, the corresponding theoretical analysis of the convergence and sample complexity is performed and validated through numerical simulations.

**Related Work.** Recent MBRL approaches are proposed to improve the data efficiency by introducing the learned dynamics, for instance, in [26–28] the authors proposed to apply the non-parametric probabilistic Gaussian processes (GPs) to approximate the system dynamics by DNN, then the (near) optimal policy is found by either modern optimal control techniques such as model predictive control (MPC) [29] or PG methods [30]. In spite of that, the above approaches are not directly applied to solve the tasks with the objective function of an infinite time horizon. In addition, these methods impose further assumptions on the system, including the assumption of smoothness that is inherent in GPs with squared-exponential kernels [27]. MBRL has also extensively utilized parametric function approximators, but Bayesian models have largely replaced them in recent years [31–34]. Local model-based methods, including guided policy search algorithms [35, 36], are capable of training DNN policies efficiently. However, these methods utilize time-varying linear models that only model the system dynamics locally. Modeling the unknown dynamics using DNN has recently proven to be helpful in RL. Authors of [29] use DNN to model the system dynamics and propose an algorithm called probabilistic ensembles with trajectory sampling (PETS).

The paper is organized as follows. In Section 2, we formulate the problem. Section 3 presents the algorithm and theoretic analysis. Then in Section 4, we validate the algorithm and analytical results through numerical simulations. Finally, Section 5 concludes the paper.

**Notations.** Let  $\|\cdot\|$  be the Euclidean norm. For a matrix  $A \in \mathbb{R}^{n \times m}$ ,  $\|A\|_F$  denotes its Frobenius norm;  $A'$  denotes its transpose;  $A^\dagger$  denotes its Moore-Penrose pseudoinverse. For positive integers  $n$  and  $m$ ,  $\mathbf{I}_n$  denotes the  $n \times n$  identity matrix;  $\mathbf{0}_n \in \mathbb{R}^n$  denotes a vector with all value 0;  $\mathbf{0}_{n \times m}$  denotes a  $n \times m$  matrix with all value 0.  $\langle \cdot, \cdot \rangle$  denotes the inner product.

## 2 Problem Formulation

Consider the following discrete-time system:

$$\begin{aligned} \text{performance index:} \quad & J_t(\mathbf{x}, \mathbf{u}) = \sum_{i=t}^{\infty} \gamma^{i-t} c(\mathbf{x}_i, \mathbf{u}_i), \\ \text{dynamics:} \quad & \mathbf{x}_{t+1} = \mathbf{f}(\mathbf{x}_t, \mathbf{u}_t), \quad \text{with } \mathbf{x}_0 \text{ given,} \end{aligned} \quad (1)$$

where  $t = 0, 1, 2, \dots$  denotes the system time index;  $\mathbf{x}_t \in \mathbb{R}^n$  and  $\mathbf{u}_t \in \mathbb{R}^m$  denote the system state and control input, respectively;  $0 < \gamma \leq 1$  is the discount factor;  $c(\mathbf{x}_t, \mathbf{u}_t) \geq 0 : \mathbb{R}^n \times \mathbb{R}^m \rightarrow \mathbb{R}$  is the stage cost and  $\mathbf{f} : \mathbb{R}^n \times \mathbb{R}^m \rightarrow \mathbb{R}^n$  denotes the system dynamics which is unknown and time-invariant.

Suppose one can observe the system states-inputs from (1) in data batches defined by:

$$\xi_\tau = \{\mathbf{x}_k, \mathbf{u}_k : k \in \mathbb{K}_\tau\}, \quad (2)$$

where  $\tau = 0, 1, 2, \dots$  denotes the batch index which is slower than  $t$ ;  $\mathbb{K}_\tau = \{t_\tau, t_\tau + 1, \dots, t_\tau + N_\tau\}$  with  $t_0$  given and  $N_\tau$  a positive integer that determines the number of the data points in  $\xi_\tau$ ;  $t_\tau$  denotes the observation time of the first data point in  $\xi_\tau$ .

The primary goal of this paper is to achieve a sequence of control inputs  $\mathbf{u} = \{\mathbf{u}_0, \mathbf{u}_1, \mathbf{u}_2, \dots\}$  that minimizes the performance index  $J_t(\mathbf{x}, \mathbf{u})$  in (1) when  $\mathbf{f}$  is unknown. Different from model-based traditional optimal control methods, which require  $\mathbf{f}$  to be known before hands, or classical model-free reinforcement learning methods, which do not need to know  $\mathbf{f}$  but rely on a predefined reward function, data-driven model-based methods have recently become popular, which first perform a nice estimate to the system dynamics based on data batches available and then develop the corresponding control policy. In this paper, we proceed in a direction similar to data-driven model-based methods but develop an innovative way to approximate both the system dynamics and the control policy at the same time. Although  $\mathbf{f}$  is unknown here, we assume it obeys the following structure  $\hat{\mathbf{f}}$  with an unknown tunable parameter  $\theta^f$  :

$$\hat{\mathbf{x}}_{t+1} = \hat{\mathbf{f}}(\hat{\mathbf{x}}_t, \mathbf{u}_t, \theta^f), \quad \text{with } \hat{\mathbf{x}}_0 \text{ given,} \quad (3)$$

where  $\hat{\mathbf{f}} : \mathbb{R}^n \times \mathbb{R}^m \times \mathbb{R}^p \rightarrow \mathbb{R}^n$  denotes an approximated dynamics with tunable parameter  $\theta^f \in \mathbb{R}^p$  to be determined later and  $\hat{\mathbf{x}}_t \in \mathbb{R}^n$  denotes the introduced system state of  $\hat{\mathbf{f}}$ . Correspondingly the optimal control policy  $\mathbf{u}_t$  is assumed to obey the following control policy:

$$\mathbf{u}_t = \mu(\mathbf{x}_t, \theta^\mu), \quad (4)$$

where  $\mu : \mathbb{R}^n \times \mathbb{R}^q \rightarrow \mathbb{R}^m$  denotes a twice-differentiable function with known structure and tunable by parameter  $\theta^\mu \in \mathbb{R}^q$ .

To sum up, the **problem of interest** is to find an update rule to tune  $\theta^f \in \mathbb{R}^p$  and  $\theta^\mu \in \mathbb{R}^q$  simultaneously only based on available  $\xi_\tau$  in (2) to achieve both of the following objectives at the same time. First, given any  $\xi_\tau = \{\mathbf{x}_k, \mathbf{u}_k : k \in \mathbb{K}_\tau\}$ ,  $\mathbb{K}_\tau = \{t_\tau, t_\tau + 1, \dots, t_\tau + N_\tau\}$  with  $\hat{\mathbf{x}}_{t_\tau} := \mathbf{x}_{t_\tau}$ <sup>3</sup>, the introduced state  $\hat{\mathbf{x}}_k$  from the approximated system dynamics in (3) is close to the observed system state  $\mathbf{x}_k$  in  $\xi_\tau$ , in the sense that for any given constant  $\epsilon \geq 0$ , one has  $\|\hat{\mathbf{x}}_k - \mathbf{x}_k\| \leq \epsilon$ . Correspondingly one aims to minimize the following loss function by tuning  $\theta^f \in \mathbb{R}^p$ :

$$\mathbf{L}_1 = \frac{1}{N_\tau} \sum_{k=t_\tau+1}^{t_\tau+N_\tau} \|\hat{\mathbf{x}}_k - \mathbf{x}_k\|^2. \quad (5)$$

Based on available  $\hat{\mathbf{x}}_k$ , which is close to  $\mathbf{x}_k$ , one performs the minimization of  $J_t(\hat{\mathbf{x}}, \mathbf{u})$  with  $\hat{\mathbf{x}}_t := \mathbf{x}_t$  (it implies that  $\hat{\mathbf{f}}$  in (3) is used to predict the future system states after time  $t$  during the minimization), which approximates the minimization of  $J_t(\mathbf{x}, \mathbf{u})$  in (1).

## 3 Main Results

In this section, we first propose a data-driven control framework that minimizes (5) and  $J_t(\mathbf{x}, \mathbf{u})$  in (1) based on  $\xi_\tau$  in (2). Then the corresponding theoretical analysis is provided. For simplicity, we define  $c_t := c(\mathbf{x}_t, \mathbf{u}_t)$  and  $J_t := J_t(\mathbf{x}, \mathbf{u})$  in the remainder of this manuscript.

<sup>3</sup>This enforces that for any data batch  $\xi_\tau$ , the initial state of  $\hat{\mathbf{f}}$  is the same as the first system state in  $\xi_\tau$

### 3.1 Key ideas

We begin with the performance index described in (1) with the admissible control input  $\mathbf{u}_t$  selected from the control policy in (4):

$$J_t = c(\mathbf{x}_t, \mathbf{u}_t) + \gamma \sum_{i=t+1}^{\infty} \gamma^{i-t-1} c(\mathbf{x}_i, \mathbf{u}_i) = c(\mathbf{x}_t, \mathbf{u}_t) + \gamma J_{t+1}. \quad (6)$$

Then by following the Bellman optimality principle, the Hamilton–Jacobi–Bellman equation of (6) becomes

$$J_t^* = \min_{\boldsymbol{\theta}^\mu \in \mathbb{R}^q} \{c(\mathbf{x}_t, \mathbf{u}_t) + \gamma J_{t+1}^*\}. \quad (7)$$

One popular way to solve (7) is by applying the gradient descent method to update the policy parameter  $\boldsymbol{\theta}^\mu$ , i.e.,

$$\boldsymbol{\theta}_{i+1}^\mu = \boldsymbol{\theta}_i^\mu - \alpha_i^\mu \left. \frac{dJ_t}{d\boldsymbol{\theta}^\mu} \right|_{\boldsymbol{\theta}_i^\mu}, \quad (8)$$

with

$$\frac{dJ_t}{d\boldsymbol{\theta}^\mu} = \frac{\partial c(\mathbf{x}_t, \mathbf{u}_t)}{\partial \mathbf{u}_t} \frac{\partial \mathbf{u}_t}{\partial \boldsymbol{\theta}^\mu} + \gamma \frac{\partial J_{t+1}}{\partial \mathbf{x}_{t+1}} \frac{\partial \mathbf{x}_{t+1}}{\partial \mathbf{u}_t} \frac{\partial \mathbf{u}_t}{\partial \boldsymbol{\theta}^\mu} + \gamma \frac{\partial J_{t+1}}{\partial \mathbf{u}_{t+1}} \frac{\partial \mathbf{u}_{t+1}}{\partial \boldsymbol{\theta}^\mu}, \quad (9)$$

where  $i = 0, 1, 2, \dots$  is the iteration index;  $\alpha_i^\mu$  denotes the step size at the  $i$ -th iteration corresponding to  $\boldsymbol{\theta}^\mu$  and  $\left. \frac{dJ_t}{d\boldsymbol{\theta}^\mu} \right|_{\boldsymbol{\theta}_i^\mu}$  denotes the gradient of  $J_t$  regarding  $\boldsymbol{\theta}^\mu$  evaluated at  $\boldsymbol{\theta}_i^\mu$ .

Toward this direction, two issues arise while solving (9). First, the dynamics of (1) is unknown, i.e.,  $\frac{\partial \mathbf{x}_{t+1}}{\partial \mathbf{u}_t}$  is not available. Furthermore,  $J_t$  in (1) is defined with an infinite time horizon, which makes it challenging to compute the  $\frac{\partial J_{t+1}}{\partial \mathbf{x}_{t+1}}$  and  $\frac{\partial J_{t+1}}{\partial \mathbf{u}_{t+1}}$  directly. To overcome these two problems, we propose the following algorithm.

### 3.2 Algorithm

To compute (9) such that one can apply the gradient descent in (8) to update the control policy  $\mu(\cdot, \boldsymbol{\theta}^\mu)$  in (4), the following approximation components about the system dynamics  $\mathbf{f}$  and performance index  $J_{t+1}$  are introduced, respectively.

#### 3.2.1 Dynamics approximation

Instead of utilizing a DNN to represent  $\hat{\mathbf{f}}$  in (3) directly, motivated by the recent work [25], in which the authors proposed to approximate the unknown nonlinear time-varying systems by a linear time-varying system based on the Koopman operator theory and DNN, this paper seeks to find the following so-called *deep Koopman representation* (DKR):

$$\mathcal{K} := \{g(\cdot, \boldsymbol{\theta}^f), A, B, C\}, \quad (10)$$

where  $g(\cdot, \boldsymbol{\theta}^f) : \mathbb{R}^n \rightarrow \mathbb{R}^r$  is a twice-differentiable mapping function represented by a DNN with  $\boldsymbol{\theta}^f \in \mathbb{R}^p$  a tunable parameter to be determined later and  $A \in \mathbb{R}^{r \times r}$ ,  $B \in \mathbb{R}^{r \times m}$ ,  $C \in \mathbb{R}^{n \times r}$  are constant matrices such that for any  $k \in \mathbb{K}_\tau$ ,  $k < t_\tau + N_\tau$  the following holds approximately:

$$\begin{aligned} g(\mathbf{x}_{k+1}, \boldsymbol{\theta}^f) &= Ag(\mathbf{x}_k, \boldsymbol{\theta}^f) + B\mathbf{u}_k, \\ \mathbf{x}_{k+1} &= Cg(\mathbf{x}_{k+1}, \boldsymbol{\theta}^f). \end{aligned}$$

Then by introducing the  $\hat{\mathbf{x}}_k \in \mathbb{R}^n$  such that for any  $k \in \mathbb{K}_\tau$ ,  $k < t_\tau + N_\tau$  with  $\hat{\mathbf{x}}_{t_\tau} = \mathbf{x}_{t_\tau}$ , the following holds,

$$\begin{aligned} g(\hat{\mathbf{x}}_{k+1}, \boldsymbol{\theta}^f) &= Ag(\hat{\mathbf{x}}_k, \boldsymbol{\theta}^f) + B\mathbf{u}_k, \\ \hat{\mathbf{x}}_{k+1} &= Cg(\hat{\mathbf{x}}_{k+1}, \boldsymbol{\theta}^f), \end{aligned}$$

which yields the following system predictor:

$$\hat{\mathbf{x}}_{k+1} = \hat{\mathbf{f}}(\hat{\mathbf{x}}_k, \mathbf{u}_k, \boldsymbol{\theta}^f) = C(Ag(\hat{\mathbf{x}}_k, \boldsymbol{\theta}^f) + B\mathbf{u}_k). \quad (11)$$

To this end, in order to achieve such  $\mathcal{K}$  in (10), one first writes the  $\xi_\tau$  in (2) in a compact form as:

$$\begin{aligned}\mathbf{X}_\tau &= [\mathbf{x}_{t_\tau}, \mathbf{x}_{t_\tau+1}, \dots, \mathbf{x}_{t_\tau+N_\tau-1}] \in \mathbb{R}^{n \times N_\tau}, \\ \bar{\mathbf{X}}_\tau &= [\mathbf{x}_{t_\tau+1}, \mathbf{x}_{t_\tau+2}, \dots, \mathbf{x}_{t_\tau+N_\tau}] \in \mathbb{R}^{n \times N_\tau}, \\ \mathbf{U}_\tau &= [\mathbf{u}_{t_\tau}, \mathbf{u}_{t_\tau+1}, \dots, \mathbf{u}_{t_\tau+N_\tau-1}] \in \mathbb{R}^{m \times N_\tau}.\end{aligned}$$

Accordingly, one defines

$$\begin{aligned}\mathbf{G}_\tau &= [g(\mathbf{x}_{t_\tau}, \boldsymbol{\theta}^f), g(\mathbf{x}_{t_\tau+1}, \boldsymbol{\theta}^f), \dots, g(\mathbf{x}_{t_\tau+N_\tau-1}, \boldsymbol{\theta}^f)] \in \mathbb{R}^{r \times N_\tau}, \\ \bar{\mathbf{G}}_\tau &= [g(\mathbf{x}_{t_\tau+1}, \boldsymbol{\theta}^f), g(\mathbf{x}_{t_\tau+2}, \boldsymbol{\theta}^f), \dots, g(\mathbf{x}_{t_\tau+N_\tau}, \boldsymbol{\theta}^f)] \in \mathbb{R}^{r \times N_\tau}.\end{aligned}\quad (12)$$

Then by substituting (11) into (5), the loss function  $\mathbf{L}_1$  in (5) can be reformulated as:

$$\min_{\boldsymbol{\theta}^f \in \mathbb{R}^p} \mathbf{L}_1 = \min_{\boldsymbol{\theta}^f \in \mathbb{R}^p} \{\mathbf{L}_{11}(A, B, \boldsymbol{\theta}^f) + \mathbf{L}_{12}(C, \boldsymbol{\theta}^f)\}, \quad (13)$$

with

$$\mathbf{L}_{11} = \frac{1}{N_\tau} \sum_{k=t_\tau}^{t_\tau+N_\tau-1} \|g(\mathbf{x}_{k+1}, \boldsymbol{\theta}^f) - Ag(\mathbf{x}_k, \boldsymbol{\theta}^f) - B\mathbf{u}_k\|^2 = \frac{1}{N_\tau} \|\bar{\mathbf{G}}_\tau - (A\mathbf{G}_\tau + B\mathbf{U}_\tau)\|_F^2 \quad (14)$$

and

$$\mathbf{L}_{12} = \frac{1}{N_\tau} \sum_{k=t_\tau}^{k_\tau+N_\tau-1} \|\mathbf{x}_k - Cg(\mathbf{x}_k, \boldsymbol{\theta}^f)\|^2 = \frac{1}{N_\tau} \|\mathbf{X}_\tau - C\mathbf{G}_\tau\|_F^2. \quad (15)$$

Here,  $\mathbf{L}_{11}$  and  $\mathbf{L}_{12}$  in (14)-(15) denote the simulation errors in the lifted and original coordinates, respectively, and to achieve a minimization solution of (14)-(15), the following assumption is made.

**Assumption 1** The matrix  $\mathbf{G}_\tau \in \mathbb{R}^{r \times N_\tau}$  in (12) and  $\begin{bmatrix} \mathbf{G}_\tau \\ \mathbf{U}_\tau \end{bmatrix} \in \mathbb{R}^{(r+m) \times N_\tau}$  are with full row ranks.

**Remark 1** Assumption 1 is to ensure the matrices  $\mathbf{G}_\tau \in \mathbb{R}^{r \times N_\tau}$  and  $\begin{bmatrix} \mathbf{G}_\tau \\ \mathbf{U}_\tau \end{bmatrix} \in \mathbb{R}^{(r+m) \times N_\tau}$  invertible and it requires  $N_\tau \geq r + m$ .

If Assumption 1 holds, by minimizing  $\mathbf{L}_{11}$  in (14) regarding the matrices  $A, B$  and minimizing  $\mathbf{L}_{12}$  (15) with respect to the matrix  $C$ , the matrices  $A, B, C$  can be determined by  $\boldsymbol{\theta}^f$  as follows:

$$[A_{\boldsymbol{\theta}^f}, B_{\boldsymbol{\theta}^f}] = \bar{\mathbf{G}}_\tau \begin{bmatrix} \mathbf{G}_\tau \\ \mathbf{U}_\tau \end{bmatrix}^\dagger, \quad (16)$$

$$C_{\boldsymbol{\theta}^f} = \mathbf{X}_\tau (\mathbf{G}_\tau)^\dagger. \quad (17)$$

Since solving pseudoinverse could be computationally expensive as  $N_\tau$  increases, in this work, we only compute (16)-(17) before updating  $\boldsymbol{\theta}^f$ . By replacing  $A, B$  in (14) by (16) and  $C$  in (15) by (17), the loss function (13) is further reduced with respect to the tunable parameter  $\boldsymbol{\theta}^f \in \mathbb{R}^p$  as:

$$\begin{aligned}\mathbf{L}_1(\boldsymbol{\theta}^f) &= \frac{1}{N_\tau} \sum_{k=t_\tau}^{t_\tau+N_\tau-1} \left\| \begin{bmatrix} g(\mathbf{x}_{k+1}, \boldsymbol{\theta}^f) \\ \mathbf{x}_k \end{bmatrix} - K(\boldsymbol{\theta}_0^f) \begin{bmatrix} g(\mathbf{x}_k, \boldsymbol{\theta}^f) \\ \mathbf{u}_k \end{bmatrix} \right\|^2 \\ &= \frac{1}{N_\tau} \left\| \begin{bmatrix} \bar{\mathbf{G}}_\tau \\ \mathbf{X}_\tau \end{bmatrix} - K(\boldsymbol{\theta}_0^f) \begin{bmatrix} \mathbf{G}_\tau \\ \mathbf{U}_\tau \end{bmatrix} \right\|_F^2,\end{aligned}\quad (18)$$

where

$$K(\boldsymbol{\theta}_0^f) = \begin{bmatrix} A_{\boldsymbol{\theta}_0^f} & B_{\boldsymbol{\theta}_0^f} \\ C_{\boldsymbol{\theta}_0^f} & \mathbf{0}_{n \times m} \end{bmatrix}.$$

Then, an optimal  $\boldsymbol{\theta}^{f*} \in \mathbb{R}^p$  that minimizes the  $\mathbf{L}_1$  in (18) can be found by performing the following gradient descent

$$\boldsymbol{\theta}_{i+1}^f = \boldsymbol{\theta}_i^f - \alpha_i^f \frac{d\mathbf{L}_1(\boldsymbol{\theta}^f)}{d\boldsymbol{\theta}^f} \Big|_{\boldsymbol{\theta}_i^f},$$

where

$$\frac{d\mathbf{L}_1(\boldsymbol{\theta}^f)}{d\boldsymbol{\theta}^f} = \frac{2}{N_\tau} \sum_{k=t_\tau}^{t_\tau+N_\tau-1} \boldsymbol{\delta}'_k \left( \begin{bmatrix} \frac{\partial g(\mathbf{x}_{k+1}, \boldsymbol{\theta}^f)}{\partial \boldsymbol{\theta}^f} \\ \mathbf{0}_n \end{bmatrix} - K(\boldsymbol{\theta}_0^f) \begin{bmatrix} \frac{\partial g(\mathbf{x}_k, \boldsymbol{\theta}^f)}{\partial \boldsymbol{\theta}^f} \\ \mathbf{0}_m \end{bmatrix} \right), \quad (19)$$

with  $\boldsymbol{\delta}_k = \begin{bmatrix} g(\mathbf{x}_{k+1}, \boldsymbol{\theta}^f) \\ \mathbf{x}_k \end{bmatrix} - K(\boldsymbol{\theta}_0^f) \begin{bmatrix} g(\mathbf{x}_k, \boldsymbol{\theta}^f) \\ \mathbf{u}_k \end{bmatrix}$  and  $\alpha_i^f$  the step size at the  $i$ -th iteration regarding  $\boldsymbol{\theta}^f$ .

### 3.2.2 Performance index approximation

Inspired by the well-known work [37], one popular way to achieve such an approximation of  $J_{t+1}$  in (9) is by minimizing the so-called temporal-difference (TD) error function defined by:

$$\min_{\boldsymbol{\theta}^J \in \mathbb{R}^l} \mathbf{L}_3 = \min_{\boldsymbol{\theta}^J \in \mathbb{R}^l} \frac{1}{N_\tau} \sum_{k=t_\tau}^{t_\tau+N_\tau-1} (c(\mathbf{x}_k, \mathbf{u}_k) + \gamma \hat{J}(\mathbf{x}_{k+1}, \boldsymbol{\theta}^J) - \hat{J}(\mathbf{x}_k, \boldsymbol{\theta}^J))^2, \quad (20)$$

where  $\hat{J}(\mathbf{x}_{t+1}, \boldsymbol{\theta}^J) : \mathbb{R}^n \times \mathbb{R}^l \rightarrow \mathbb{R}$  denotes a twice-differentiable function to approximate  $J_{t+1}$ , which is defined with a known structure and tunable parameter  $\boldsymbol{\theta}^J \in \mathbb{R}^l$ . Then the optimal  $\boldsymbol{\theta}^{J*}$  that minimizes (20) can be found by performing the gradient descent

$$\boldsymbol{\theta}_{i+1}^J = \boldsymbol{\theta}_i^J - \alpha_i^J \frac{d\mathbf{L}_3(\boldsymbol{\theta}^J)}{d\boldsymbol{\theta}^J} \Big|_{\boldsymbol{\theta}_i^J}, \quad (21)$$

where

$$\frac{d\mathbf{L}_3(\boldsymbol{\theta}^J)}{d\boldsymbol{\theta}^J} = \frac{2}{N_\tau} \sum_{k=t_\tau}^{t_\tau+N_\tau-1} \hat{\delta}_k \left( \gamma \frac{\partial \hat{J}(\mathbf{x}_{k+1}, \boldsymbol{\theta}^J)}{\partial \boldsymbol{\theta}^J} - \frac{\partial \hat{J}(\mathbf{x}_k, \boldsymbol{\theta}^J)}{\partial \boldsymbol{\theta}^J} \right), \quad (22)$$

with  $\hat{\delta}_k = c(\mathbf{x}_k, \mathbf{u}_k) + \gamma \hat{J}(\mathbf{x}_{k+1}, \boldsymbol{\theta}^J) - \hat{J}(\mathbf{x}_k, \boldsymbol{\theta}^J)$  and  $\alpha_i^J$  denotes the step size at the  $i$ -th iteration with respect to  $\boldsymbol{\theta}^J \in \mathbb{R}^l$ . Since TD error learning is a well-studied method we refer to the popular work [38] for more details of its theoretic analysis.

### 3.2.3 Policy update

To achieve the optimal policy that minimizes  $J_t$  in (1) based on  $\xi_\tau$  in (2), one can define the following loss function  $\mathbf{L}_2$  as an approximated function of  $J_t$  by following (7) with its  $J_{t+1}$  replaced by  $\hat{J}(\hat{\mathbf{x}}_{t+1}, \boldsymbol{\theta}^J)$  from (20):

$$\min_{\boldsymbol{\theta}^\mu \in \mathbb{R}^q} \mathbf{L}_2 = \min_{\boldsymbol{\theta}^\mu \in \mathbb{R}^q} \frac{1}{N_\tau} \sum_{k=t_\tau}^{t_\tau+N_\tau-1} c(\mathbf{x}_k, \mathbf{u}_k) + \gamma \hat{J}(\hat{\mathbf{x}}_{k+1}, \boldsymbol{\theta}^J), \quad \text{with } \hat{\mathbf{x}}_{t_\tau} = \mathbf{x}_{t_\tau}. \quad (23)$$

Then  $\boldsymbol{\theta}^\mu \in \mathbb{R}^q$  is updated using the policy gradient

$$\boldsymbol{\theta}_{i+1}^\mu = \boldsymbol{\theta}_i^\mu - \alpha_i^\mu \frac{d\mathbf{L}_2}{d\boldsymbol{\theta}^\mu} \Big|_{\boldsymbol{\theta}_{i+1}^f, \boldsymbol{\theta}_{i+1}^J, \boldsymbol{\theta}_i^\mu} \quad (24)$$

with

$$\frac{d\mathbf{L}_2}{d\boldsymbol{\theta}^\mu} = \frac{1}{N_\tau} \sum_{k=t_\tau}^{t_\tau+N_\tau-1} \frac{\partial c(\mathbf{x}_k, \mathbf{u}_k)}{\partial \mathbf{u}_k} \frac{\partial \mathbf{u}_k}{\partial \boldsymbol{\theta}^\mu} + \gamma \frac{\partial \hat{J}(\hat{\mathbf{x}}_{k+1}, \boldsymbol{\theta}^J)}{\partial \hat{\mathbf{x}}_{k+1}} \frac{\partial \hat{\mathbf{x}}_{k+1}}{\partial \mathbf{u}_k} \frac{\partial \mathbf{u}_k}{\partial \boldsymbol{\theta}^\mu}. \quad (25)$$

Here,  $\frac{\partial \hat{\mathbf{x}}_{k+1}}{\partial \mathbf{u}_k} = C_{\boldsymbol{\theta}_0^f} B_{\boldsymbol{\theta}_0^f}$  with  $B_{\boldsymbol{\theta}_0^f} \in \mathbb{R}^{r \times m}$  and  $C_{\boldsymbol{\theta}_0^f} \in \mathbb{R}^{n \times r}$  computed by (16) and (17), respectively, as indicated by (11). Note that since the minimization of  $\mathbf{L}_2$  is based on the approximated dynamics and approximated performance index, and the minimization of both  $\mathbf{L}_2$  and  $\mathbf{L}_3$  require the approximated dynamics for state prediction, it is reasonable to assign the convergence order of the above three components, i.e., the approximation of the dynamics converges first, followed by the performance index approximation, and then finally the policy. One way to achieve this is to set  $\alpha_i^f > \alpha_i^J > \alpha_i^\mu$  (shown in Fig. ??). The pseudocode is summarized in Algorithm 1.

### 3.3 Analysis

In this subsection, an analysis of the convergence rates with respect to  $\mathbf{L}_1$ ,  $\mathbf{L}_2$ , and sample complexity of Algorithm 1 is provided. For brevity, given an arbitrary function  $\mathbf{f}(\mathbf{x}, \mathbf{y})$ ,  $\nabla_{\mathbf{x}} \mathbf{f}(\mathbf{x}_k) := \frac{\partial \mathbf{f}(\mathbf{x}, \mathbf{y})}{\partial \mathbf{x}} \Big|_{\mathbf{x}_k}$  and  $\nabla_{\mathbf{x}\mathbf{x}} \mathbf{f}(\mathbf{x}_k) := \frac{\partial^2 \mathbf{f}(\mathbf{x}, \mathbf{y})}{\partial \mathbf{x} \partial \mathbf{x}} \Big|_{\mathbf{x}_k}$  denote the first-order and second-order partial derivative of  $\mathbf{f}(\mathbf{x}, \mathbf{y})$  with respect to  $\mathbf{x}$  evaluated at  $\mathbf{x}_k$ , respectively, similarly, let  $\nabla_{\mathbf{x}\mathbf{y}} \mathbf{f}(\mathbf{x}_k, \mathbf{y}_k) := \frac{\partial^2 \mathbf{f}(\mathbf{x}, \mathbf{y})}{\partial \mathbf{x} \partial \mathbf{y}} \Big|_{\mathbf{x}_k, \mathbf{y}_k}$  denote the second-order derivative of  $\mathbf{f}(\mathbf{x}, \mathbf{y})$  evaluated at  $(\mathbf{x}_k, \mathbf{y}_k)$  in the remainder of this manuscript.

To conduct the analysis, it is necessary to assume that there exist optimal solutions that minimize the loss functions  $\mathbf{L}_1$  in (18),  $\mathbf{L}_2$  in (23), and  $\mathbf{L}_3$  in (20). Additionally, the functions  $c(\mathbf{x}_t, \mathbf{u}_t)$  in (1),  $g(\cdot, \boldsymbol{\theta}^f)$  in (10),  $\mu(\cdot, \boldsymbol{\theta}^\mu)$  in (4), and  $\hat{J}(\cdot, \boldsymbol{\theta}^J)$  in (20) need to satisfy the condition of being Lipschitz continuous, for which we make the following technical assumptions.

---

**Algorithm 1:** Policy Gradient-based on Deep Koopman Representation (PGDK)

---

Initialize  $g(\mathbf{x}, \boldsymbol{\theta}^f)$ ,  $\mu(\mathbf{x}, \boldsymbol{\theta}^\mu)$ ,  $\hat{J}(\mathbf{x}, \boldsymbol{\theta}^J)$  with  $\boldsymbol{\theta}_0^f \in \mathbb{R}^p$ ,  $\boldsymbol{\theta}_0^\mu \in \mathbb{R}^q$ ,  $\boldsymbol{\theta}_0^J \in \mathbb{R}^l$ , respectively and compute  $A_{\boldsymbol{\theta}_0^f}$ ,  $B_{\boldsymbol{\theta}_0^f}$  and  $C_{\boldsymbol{\theta}_0^f}$  by (16) and (17), respectively.

Initialize the iteration index  $i = 0$ , learning rate sequences  $\{\alpha_i^f\}_{i=0}^T$ ,  $\{\alpha_i^\mu\}_{i=0}^T$ ,  $\{\alpha_i^J\}_{i=0}^T$  with  $\alpha_i^f > \alpha_i^J > \alpha_i^\mu$ , discount factor  $\gamma$ , number of episodes  $E$ , task horizon  $T_h$ , batch size  $N_\tau := N$  and the replay buffer  $\mathcal{D}$ .

**for** episode = 1, 2,  $\dots$ ,  $E$  **do**

**for**  $t = 0, 1, \dots, T_h$  **do**

    Execute the control input  $\mathbf{u}_t = \mu(\mathbf{x}_t, \boldsymbol{\theta}_t^\mu)$  and observe the resulting  $c_t$  and  $\mathbf{x}_{t+1}$ .

    Store the observed data tuple  $\{\mathbf{x}_t, \mathbf{u}_t, c_t, \mathbf{x}_{t+1}\}$  in  $\mathcal{D}$ .

    Sample  $N$  data tuples from  $\mathcal{D}$ , construct the data batch (2), and define the loss functions

$\mathbf{L}_1$  in (18),  $\mathbf{L}_2$  in (23), and  $\mathbf{L}_3$  in (20).

    Compute  $\frac{d\mathbf{L}_1}{d\boldsymbol{\theta}^f}$  in (19),  $\frac{d\mathbf{L}_1}{d\boldsymbol{\theta}^J}$  in (22) and update  $\boldsymbol{\theta}_i^f$ ,  $\boldsymbol{\theta}_i^J$  by:

$$\boldsymbol{\theta}_{i+1}^f = \boldsymbol{\theta}_i^f - \alpha_i^f \frac{d\mathbf{L}_1}{d\boldsymbol{\theta}^f} \Big|_{\boldsymbol{\theta}_i^f},$$

$$\boldsymbol{\theta}_{i+1}^J = \boldsymbol{\theta}_i^J - \alpha_i^J \frac{d\mathbf{L}_3}{d\boldsymbol{\theta}^J} \Big|_{\boldsymbol{\theta}_i^J}.$$

    Compute  $\frac{d\mathbf{L}_2}{d\boldsymbol{\theta}^\mu}$  in (25) and update  $\boldsymbol{\theta}_i^\mu$  by:

$$\boldsymbol{\theta}_{i+1}^\mu = \boldsymbol{\theta}_i^\mu - \alpha_i^\mu \frac{d\mathbf{L}_2}{d\boldsymbol{\theta}^\mu} \Big|_{\boldsymbol{\theta}_{i+1}^f, \boldsymbol{\theta}_{i+1}^J, \boldsymbol{\theta}_i^\mu}.$$

$i = i + 1$

**end**

**end**

---

**Assumption 2** There exist optimal parameters  $\boldsymbol{\theta}^{f*} \in \mathbb{R}^p$ ,  $\boldsymbol{\theta}^{J*} \in \mathbb{R}^l$  and  $\boldsymbol{\theta}^{\mu*} \in \mathbb{R}^q$ , such that  $\mathbf{L}_1(\boldsymbol{\theta}^{f*}) = 0$ ,  $\mathbf{L}_3(\boldsymbol{\theta}^{J*}) = 0$ , and  $\boldsymbol{\theta}^{\mu*} \in \arg \min_{\boldsymbol{\theta}^\mu \in \mathbb{R}^q} \mathbf{L}_2(\boldsymbol{\theta}^f, \boldsymbol{\theta}^J, \boldsymbol{\theta}^\mu)$ , respectively.

**Assumption 3**  $\forall \mathbf{x}_1, \mathbf{x}_2 \in \mathbb{R}^n$ , there exist positive constants  $L_{Jx}$  and  $L_{Jxx}$  such that  $|\hat{J}(\mathbf{x}_1, \boldsymbol{\theta}^J) - \hat{J}(\mathbf{x}_2, \boldsymbol{\theta}^J)| \leq L_{Jx} \|\mathbf{x}_1 - \mathbf{x}_2\|$  and  $|\nabla_{\mathbf{x}} \hat{J}(\mathbf{x}_1) - \nabla_{\mathbf{x}} \hat{J}(\mathbf{x}_2)| \leq L_{Jxx} \|\mathbf{x}_1 - \mathbf{x}_2\|$ , respectively.  $\forall \mathbf{u}_1, \mathbf{u}_2 \in \mathbb{R}^m$ , there exist positive constants  $L_{cu}$  and  $L_{cuu}$  such that  $|c(\mathbf{x}, \mathbf{u}_1) - c(\mathbf{x}, \mathbf{u}_2)| \leq L_{cu} \|\mathbf{u}_1 - \mathbf{u}_2\|$  and  $|\nabla_{\mathbf{u}} c(\mathbf{u}_1) - \nabla_{\mathbf{u}} c(\mathbf{u}_2)| \leq L_{cuu} \|\mathbf{u}_1 - \mathbf{u}_2\|$ , respectively.  $\forall \boldsymbol{\theta}_1^f, \boldsymbol{\theta}_2^f \in \mathbb{R}^p$ , there exists positive constant  $L_{g\theta}$  such that  $\|g(\mathbf{x}, \boldsymbol{\theta}_1^f) - g(\mathbf{x}, \boldsymbol{\theta}_2^f)\| \leq L_{g\theta} \|\boldsymbol{\theta}_1^f - \boldsymbol{\theta}_2^f\|$ .  $\forall \boldsymbol{\theta}_1^\mu, \boldsymbol{\theta}_2^\mu \in \mathbb{R}^q$ , there exist positive constants  $L_{\mu\theta}$  and  $L_{\mu\theta\theta}$  such that  $\|\mu(\mathbf{x}, \boldsymbol{\theta}_1^\mu) - \mu(\mathbf{x}, \boldsymbol{\theta}_2^\mu)\| \leq L_{\mu\theta} \|\boldsymbol{\theta}_1^\mu - \boldsymbol{\theta}_2^\mu\|$  and  $\|\nabla_{\boldsymbol{\theta}^\mu} \mu(\boldsymbol{\theta}_1^\mu) - \nabla_{\boldsymbol{\theta}^\mu} \mu(\boldsymbol{\theta}_2^\mu)\| \leq L_{\mu\theta\theta} \|\boldsymbol{\theta}_1^\mu - \boldsymbol{\theta}_2^\mu\|$ , respectively.

Based on the above assumptions, we have the following results.

**Lemma 1** If Assumption 3 holds, then for any  $\boldsymbol{\theta}_1^\mu, \boldsymbol{\theta}_2^\mu \in \mathbb{R}^q$  and  $\mathbf{L}_2$  in (23),  $\nabla_{\boldsymbol{\theta}^\mu} \mathbf{L}_2$  is Lipschitz continuous with positive Lipschitz constant  $L_2^{\theta\theta}$ , i.e.,

$$\|\nabla_{\boldsymbol{\theta}^\mu} \mathbf{L}_2(\boldsymbol{\theta}_1^\mu) - \nabla_{\boldsymbol{\theta}^\mu} \mathbf{L}_2(\boldsymbol{\theta}_2^\mu)\| \leq L_2^{\theta\theta} \|\boldsymbol{\theta}_1^\mu - \boldsymbol{\theta}_2^\mu\|,$$

where  $L_2^{\theta\theta} = L_{cu} L_{\mu\theta\theta} + L_{cuu} L_{\mu\theta}^2 + \gamma L_{Jx} L_{\mu\theta\theta} \|C_{\boldsymbol{\theta}_0^f} B_{\boldsymbol{\theta}_0^f}\| + \gamma L_{Jxx} L_{\mu\theta}^2 \|C_{\boldsymbol{\theta}_0^f} B_{\boldsymbol{\theta}_0^f}\|^2$ ;  $\gamma$  is the discount factor;  $B_{\boldsymbol{\theta}_0^f}, C_{\boldsymbol{\theta}_0^f}$  are computed by (16)-(17), respectively.

Proof of Lemma 1 is provided in Appendix ??.

**Lemma 2** Given a matrix  $A \in \mathbb{R}^{n \times m}$ , let  $\sigma(\cdot)$  be the singular values,  $P_k$  be the orthogonal projector onto the left singular vector subspace of  $A$  corresponding to  $\sigma(A)$ . If  $P_k \bar{\mathbf{G}}_\tau \neq 0$ ,  $P_k \mathbf{X}_\tau \neq 0$ , and under the same assumptions as in Lemma 1, for any  $\boldsymbol{\theta}_1^f, \boldsymbol{\theta}_2^f \in \mathbb{R}^p$  and  $\mathbf{L}_1$  in (18), one has

$$\|\nabla_{\boldsymbol{\theta}^f} \mathbf{L}_1(\boldsymbol{\theta}_1^f) - \nabla_{\boldsymbol{\theta}^f} \mathbf{L}_1(\boldsymbol{\theta}_2^f)\| \leq L_1^{\theta\theta} \|\boldsymbol{\theta}_1^f - \boldsymbol{\theta}_2^f\|,$$

where  $L_1^{\theta\theta} = 2(L_{g\theta}(1 + \|K(\theta_0^f)\|)^2 + 2C_1L_{g\theta\theta}(1 + \|K(\theta_0^f)\|))$  with  $C_1 = \sigma_{\min}([\bar{\mathbf{G}}_\tau, \bar{\mathbf{G}}_\tau\alpha_1])\{\alpha_1^{-2} + \frac{\|A\theta_0^f, B\theta_0^f\|^2}{1-\bar{\delta}(\alpha_1)^2}\}^{1/2} + \sigma_{\min}([\bar{\mathbf{G}}_\tau, \mathbf{X}_\tau\alpha_2])\{\alpha_2^{-2} + \frac{\|C\theta_0^f\|^2}{1-\bar{\delta}(\alpha_2)^2}\}^{1/2}$  and  $\alpha_1 > 0, \alpha_2 > 0, \bar{\delta}(\alpha_1) = \frac{\sigma_{\min}([\bar{\mathbf{G}}_\tau, \bar{\mathbf{G}}_\tau\alpha_1])}{\sigma_{\min}(\bar{\mathbf{G}}_\tau)} < 1, \bar{\delta}(\alpha_2) = \frac{\sigma_{\min}([\bar{\mathbf{G}}_\tau, \mathbf{X}_\tau\alpha_2])}{\sigma_{\min}(\bar{\mathbf{G}}_\tau)} < 1$ ;  $\bar{\mathbf{G}}_\tau$  is defined in (12) and  $K(\theta_0^f)$  is defined in (18).

Proof of Lemma 2 is given in Appendix ???. Lemmas 1-2 state that with Assumption 3 hold, the loss functions  $\mathbf{L}_1$  and  $\mathbf{L}_2$  are Lipschitz continuous. Based on this, one has the following important results about the convergence rates of  $\mathbf{L}_1$  and  $\mathbf{L}_2$ .

**Lemma 3** *If Assumptions 1-2 hold, then  $\mathbf{L}_1$  in (18) satisfies*

$$\min_{i \in \{0,1,2,\dots,T\}} \|\nabla_{\theta^f} \mathbf{L}_1(\theta_i^f)\|^2 \leq \frac{-1}{T\lambda_i^f} C_1^2,$$

where  $\lambda_i^f = -\alpha_i^f + \frac{(\alpha_i^f)^2}{2} L_1^{\theta\theta}$  with  $L_1^{\theta\theta}$  defined in Lemma 2 and  $0 < \alpha_i^f < \frac{2}{L_1^{\theta\theta}}$  and  $C_1$  is defined in Lemma 2.

Proof of Lemma 3 is given in Appendix ???. Lemma 3 shows that the convergence rate of  $\mathbf{L}_1$  is with  $\mathcal{O}(1/T)$ . For more details of the comparison between the deep Koopman Representation and its related methods refer to [25].

Since the proposed algorithm assigns the convergence order by setting  $\alpha_i^f > \alpha_i^J > \alpha_i^\mu$ , then  $\mathbf{L}_2$  determines the convergence rate of Algorithm 1. Thus the convergence behavior of  $\mathbf{L}_2$  is investigated and shown as follows.

**Theorem 1** *If Assumptions 1-2 hold, then for  $\mathbf{L}_2$  in (23), when  $\theta_i^f \neq \theta^{f*}, \theta_i^J \neq \theta^{J*}$ , one has*

$$\min_{i \in \{0,1,2,\dots,T\}} \|\nabla_{\theta^\mu} \mathbf{L}_2(\theta_i^\mu)\|^2 \leq \frac{-1}{\lambda_i^\mu} \left( \frac{L_{cu}L_{\mu\theta}}{T} + \gamma L_{Jx}L_{\mu\theta} \|C_{\theta_0^f}B_{\theta_0^f}\| \right) \|\theta_0^\mu - \theta^{\mu*}\|, \quad (26)$$

where  $\lambda_i^\mu = -\alpha_i^\mu + \frac{(\alpha_i^\mu)^2}{2} L_2^{\theta\theta}$  with  $L_2^{\theta\theta}$  defined in Lemma 1 and  $0 < \alpha_i^\mu < \frac{2}{L_2^{\theta\theta}}$ . Here, if  $\theta_i^f = \theta^{f*}, \theta_i^J \neq \theta^{J*}$ , one needs to replace  $C_{\theta_0^f}B_{\theta_0^f}$  in (26) with  $C_{\theta^{f*}}B_{\theta^{f*}}$ . Importantly, if  $\theta_i^f = \theta^{f*}, \theta_i^J = \theta^{J*}$ , then one has

$$\min_{i \in \{0,1,2,\dots,T\}} \|\nabla_{\theta^\mu} \mathbf{L}_2(\theta_i^\mu)\|^2 \leq \frac{-1}{T\lambda_i^\mu} L_{\mu\theta} (L_{cu} + \gamma L_{Jx} \|C_{\theta^{f*}}B_{\theta^{f*}}\|) \|\theta_0^\mu - \theta^{\mu*}\|.$$

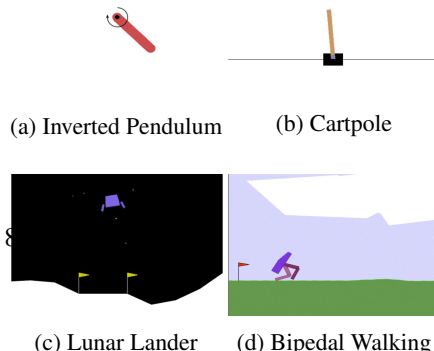
Proof of Theorem 1 is referred to Appendix ???. Theorem 1 states the convergence behavior of  $\mathbf{L}_2$  with respect to  $\theta_i^\mu$ , which is later validated by numerical simulations. Importantly, this leads to the following corollary regarding the sample complexity of Algorithm 1.

**Corollary 1** *If assumptions in Theorem 1 hold, then to achieve the stationary policy with accuracy  $\epsilon > 0$ , the proposed algorithm needs to use the total number of samples  $3TN = \mathcal{O}(1/\epsilon)$  with convergence rate  $\mathcal{O}(1/T)$ , where  $T$  and  $N$  denote the total number of gradient descent iterations and number of data points in one data batch, respectively.*

Proof of Corollary 1 is given in Appendix ???. Corollary 1 states the sample complexity of the proposed algorithm, which is supported by the following numerical simulation results.

## 4 Numerical Simulations

In this section, we demonstrate the performance of the proposed *PGDK* algorithm 1 on four standard benchmark tasks from OpenAI Gym [39], all with continuous state and control space. Then, we compare the proposed algorithm with two representative RL algorithms: (1) Deep Deterministic Policy Gradient (DDPG) [21], a well-known actor-critic MFRL algorithm; (2) Probabilistic Ensembles with Trajectory Sampling





(PETS) [29], an MBRL method that combines uncertainty-aware deep network dynamics models with sampling-based uncertainty propagation by model predictive control (MPC). An illustration of the simulation environments is shown in Fig. 1, i.e., Inverted pendulum (Fig.1a), Cartpole (Fig.1b), Lunar lander (Fig.1c) and Bipedal walking (Fig.1d).

#### 4.1 Result analysis

The comparison results are illustrated in Fig.2, in which the policy learning curves of the proposed PGDK algorithm and its comparison algorithms are exhibited. Since this work does not focus on achieving the globally optimal policy, for implementation, we add the execution noise to the control inputs to escape some local minimum solutions, and we refer to Appendix ?? for more details of the simulation setup such as the convergence behavior regarding  $\theta_i^f$ ,  $\theta_i^J$ , and  $\theta_i^H$  in Fig. ??, training parameters (e.g., noise distribution, discount factor, learning rates, etc.), DNNs architecture and other simulation examples due to the space limitations.

As can be seen, for all four benchmark tasks, the proposed PGDK is able to reach DDPG’s asymptotic performance but with better data efficiency since it requires fewer episodes to find the optimal policy as indicated in Section 3.3. Moreover, as shown in Fig.2d, the difference in average step reward between these two methods is even larger for the bipedal walking task, where the model dynamics are more complicated. When compared to PETS, PGDK can achieve similar performance but with worse data efficiency for inverted pendulum and cartpole tasks, which have simple system dynamics and tasks, and so it allows PETS to directly compute a solution to the optimal control problem instead of searching for the optimal policy. However, when the system dynamics and the tasks become more complicated (e.g., the lunar lander (Fig. 2c) and bipedal walking tasks 2d), the PETS model of system dynamics is not accurate enough for PETS to find the optimal solution. Since, for complicated tasks, the desired time horizon could be huge, small inaccuracies in the model of dynamics may lead to large accumulated approximation errors along the time horizon. Also, the complex dynamics may lead to the curse of dimensionality for PETS while solving the MPC problem, where the high dimensionality of the problem makes finding a solution computationally challenging. In contrast, PGDK utilizes the DKR to learn the complicated dynamics in a linear form with convergence analysis given in [25]. Furthermore, by applying Bellman’s principle of optimality, PGDK only needs to utilize the DKR to predict one-time steps ahead, thereby avoiding accumulative estimation errors along the task time horizon.

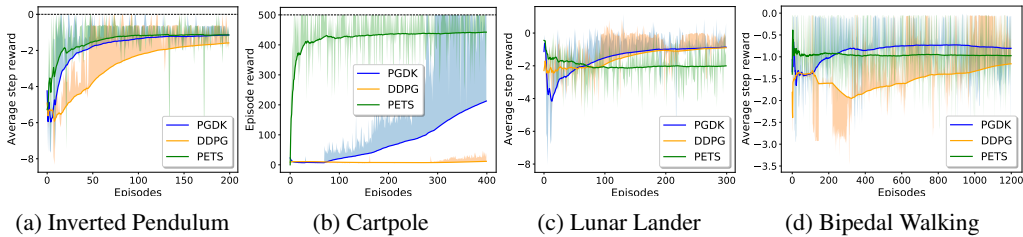


Figure 2: Learning curves of PGDK and comparison algorithms. For (a,c,d), the shadow denotes the average step reward of each episode to account for the effect of different initial states, and for (b), the shadow denotes the episode reward of each episode since the cartpole is defined with a fixed discrete step reward. The solid lines denote the accumulative average.

## 5 Conclusions

This paper proposes a policy learning methodology named Policy Gradient with Deep Koopman representation (PGDK). The key contribution of PGDK is that it utilizes the deep Koopman representation and policy gradient with TD learning to approximate the system dynamics and performance index and learn the optimal policy simultaneously. Such a combination improves the data efficiency

and convergence efficiency when compared with the existing deterministic policy gradient methods. The proposed approach has also shown the improved capability to deal with complex dynamical systems, especially for long-term tasks, when compared with the existing MBRL approaches, which combine DNN models of system dynamics and conventional optimal control techniques. Furthermore, theoretical analysis of the data efficiency of PGDK is provided and then supported by numerical simulations. An interesting direction for future work could be to extend our work to the multi-agent setting, similar to works in [40–42], with the aim of improving data efficiency in that setting.

## References

- [1] Florian Böhm, Yang Gao, Christian M Meyer, Ori Shapira, Ido Dagan, and Iryna Gurevych. Better rewards yield better summaries: Learning to summarise without references. *arXiv preprint arXiv:1909.01214*, 2019. 1
- [2] Daniel M Ziegler, Nisan Stiennon, Jeffrey Wu, Tom B Brown, Alec Radford, Dario Amodei, Paul Christiano, and Geoffrey Irving. Fine-tuning language models from human preferences. *arXiv preprint arXiv:1909.08593*, 2019.
- [3] Tom Brown, Benjamin Mann, Nick Ryder, Melanie Subbiah, Jared D Kaplan, Prafulla Dhariwal, Arvind Neelakantan, Pranav Shyam, Girish Sastry, Amanda Askell, et al. Language models are few-shot learners. *Advances in neural information processing systems*, 33:1877–1901, 2020.
- [4] Nisan Stiennon, Long Ouyang, Jeffrey Wu, Daniel Ziegler, Ryan Lowe, Chelsea Voss, Alec Radford, Dario Amodei, and Paul F Christiano. Learning to summarize with human feedback. *Advances in Neural Information Processing Systems*, 33:3008–3021, 2020.
- [5] Long Ouyang, Jeffrey Wu, Xu Jiang, Diogo Almeida, Carroll Wainwright, Pamela Mishkin, Chong Zhang, Sandhini Agarwal, Katarina Slama, Alex Ray, et al. Training language models to follow instructions with human feedback. *Advances in Neural Information Processing Systems*, 35:27730–27744, 2022. 1
- [6] Shixiang Gu, Ethan Holly, Timothy Lillicrap, and Sergey Levine. Deep reinforcement learning for robotic manipulation with asynchronous off-policy updates. In *2017 IEEE international conference on robotics and automation (ICRA)*, pages 3389–3396. IEEE, 2017. 1
- [7] Tao Chen, Adithyavairavan Murali, and Abhinav Gupta. Hardware conditioned policies for multi-robot transfer learning. *Advances in Neural Information Processing Systems*, 31, 2018.
- [8] Ilge Akkaya, Marcin Andrychowicz, Maciek Chociej, Mateusz Litwin, Bob McGrew, Arthur Petron, Alex Paino, Matthias Plappert, Glenn Powell, Raphael Ribas, et al. Solving rubik’s cube with a robot hand. *arXiv preprint arXiv:1910.07113*, 2019.
- [9] Henry Zhu, Abhishek Gupta, Aravind Rajeswaran, Sergey Levine, and Vikash Kumar. Dexterous manipulation with deep reinforcement learning: Efficient, general, and low-cost. In *2019 International Conference on Robotics and Automation (ICRA)*, pages 3651–3657. IEEE, 2019.
- [10] Yifei Simon Shao, Chao Chen, Shreyas Kousik, and Ram Vasudevan. Reachability-based trajectory safeguard (rts): A safe and fast reinforcement learning safety layer for continuous control. *IEEE Robotics and Automation Letters*, 6(2):3663–3670, 2021.
- [11] Mahmoud Selim, Amr Alanwar, Shreyas Kousik, Grace Gao, Marco Pavone, and Karl H Johansson. Safe reinforcement learning using black-box reachability analysis. *IEEE Robotics and Automation Letters*, 7(4):10665–10672, 2022. 1
- [12] Volodymyr Mnih, Koray Kavukcuoglu, David Silver, Alex Graves, Ioannis Antonoglou, Daan Wierstra, and Martin Riedmiller. Playing atari with deep reinforcement learning. *arXiv preprint arXiv:1312.5602*, 2013. 1
- [13] David Silver, Aja Huang, Chris J Maddison, Arthur Guez, Laurent Sifre, George Van Den Driessche, Julian Schrittwieser, Ioannis Antonoglou, Veda Panneershelvam, Marc Lanctot, et al. Mastering the game of go with deep neural networks and tree search. *Nature*, 529(7587):484–489, 2016.

- [14] Oriol Vinyals, Igor Babuschkin, Wojciech M Czarnecki, Michaël Mathieu, Andrew Dudzik, Junyoung Chung, David H Choi, Richard Powell, Timo Ewalds, Petko Georgiev, et al. Grandmaster level in starcraft ii using multi-agent reinforcement learning. *Nature*, 575(7782):350–354, 2019.
- [15] Bowen Baker, Ilge Akkaya, Peter Zhokov, Joost Huizinga, Jie Tang, Adrien Ecoffet, Brandon Houghton, Raul Sampedro, and Jeff Clune. Video pretraining (vpt): Learning to act by watching unlabeled online videos. *Advances in Neural Information Processing Systems*, 35:24639–24654, 2022. 1
- [16] Richard S Sutton, David McAllester, Satinder Singh, and Yishay Mansour. Policy gradient methods for reinforcement learning with function approximation. *Advances in Neural Information Processing Systems*, 12, 1999. 1
- [17] Ronald J Williams. Simple statistical gradient-following algorithms for connectionist reinforcement learning. *Reinforcement Learning*, pages 5–32, 1992. 1
- [18] Volodymyr Mnih, Koray Kavukcuoglu, David Silver, Andrei A Rusu, Joel Veness, Marc G Bellemare, Alex Graves, Martin Riedmiller, Andreas K Fidjeland, Georg Ostrovski, et al. Human-level control through deep reinforcement learning. *Nature*, 518(7540):529–533, 2015. 1
- [19] John Schulman, Filip Wolski, Prafulla Dhariwal, Alec Radford, and Oleg Klimov. Proximal policy optimization algorithms. *arXiv preprint arXiv:1707.06347*, 2017. 1
- [20] Vijaymohan R Konda and Vivek S Borkar. Actor-critic-type learning algorithms for markov decision processes. *SIAM Journal on control and Optimization*, 38(1):94–123, 1999. 1
- [21] Timothy P Lillicrap, Jonathan J Hunt, Alexander Pritzel, Nicolas Heess, Tom Erez, Yuval Tassa, David Silver, and Daan Wierstra. Continuous control with deep reinforcement learning. *arXiv preprint arXiv:1509.02971*, 2015. 1, 8
- [22] David Silver, Guy Lever, Nicolas Heess, Thomas Degris, Daan Wierstra, and Martin Riedmiller. Deterministic policy gradient algorithms. In *International conference on machine learning*, pages 387–395. Pmlr, 2014. 1
- [23] Huaqing Xiong, Tengyu Xu, Lin Zhao, Yingbin Liang, and Wei Zhang. Deterministic policy gradient: Convergence analysis. In *Uncertainty in Artificial Intelligence*, pages 2159–2169. PMLR, 2022. 1
- [24] Athanasios S Polydoros and Lazaros Nalpantidis. Survey of model-based reinforcement learning: Applications on robotics. *Journal of Intelligent & Robotic Systems*, 86(2):153–173, 2017. 2
- [25] Wenjian Hao, Bowen Huang, Wei Pan, Di Wu, and Shaoshuai Mou. Deep koopman representation of nonlinear time varying systems. *arXiv preprint arXiv:2210.06272*, 2022. 2, 4, 8, 9
- [26] Marc Peter Deisenroth, Carl Edward Rasmussen, and Jan Peters. Gaussian process dynamic programming. *Neurocomputing*, 72(7-9):1508–1524, 2009. 2
- [27] Malte Kuss and Carl Rasmussen. Gaussian processes in reinforcement learning. *Advances in neural information processing systems*, 16, 2003. 2
- [28] Marc Deisenroth and Carl E Rasmussen. Pilco: A model-based and data-efficient approach to policy search. In *Proceedings of the 28th International Conference on machine learning (ICML-11)*, pages 465–472, 2011. 2
- [29] Kurtland Chua, Roberto Calandra, Rowan McAllister, and Sergey Levine. Deep reinforcement learning in a handful of trials using probabilistic dynamics models. *Advances in neural information processing systems*, 31, 2018. 2, 9
- [30] Marc Peter Deisenroth, Carl Edward Rasmussen, and Dieter Fox. Learning to control a low-cost manipulator using data-efficient reinforcement learning. *Robotics: Science and Systems VII*, 7:57–64, 2011. 2

- [31] Evelio Hernandaz and Yaman Arkun. Neural network modeling and an extended dmc algorithm to control nonlinear systems. In *1990 American Control Conference*, pages 2454–2459. IEEE, 1990. 2
- [32] W.T. Miller, R.P. Hewes, F.H. Glanz, and L.G. Kraft. Real-time dynamic control of an industrial manipulator using a neural network-based learning controller. *IEEE Transactions on Robotics and Automation*, 6(1):1–9, 1990.
- [33] Long-Ji Lin. *Reinforcement learning for robots using neural networks*. Carnegie Mellon University, 1992.
- [34] A. Draeger, S. Engell, and H. Ranke. Model predictive control using neural networks. *IEEE Control Systems Magazine*, 15(5):61–66, 1995. 2
- [35] Yevgen Chebotar, Karol Hausman, Marvin Zhang, Gaurav Sukhatme, Stefan Schaal, and Sergey Levine. Combining model-based and model-free updates for trajectory-centric reinforcement learning. In *International conference on machine learning*, pages 703–711. PMLR, 2017. 2
- [36] Sergey Levine, Chelsea Finn, Trevor Darrell, and Pieter Abbeel. End-to-end training of deep visuomotor policies. *The Journal of Machine Learning Research*, 17(1):1334–1373, 2016. 2
- [37] Richard S Sutton. Learning to predict by the methods of temporal differences. *Machine learning*, 3:9–44, 1988. 6
- [38] Jalaj Bhandari, Daniel Russo, and Raghav Singal. A finite time analysis of temporal difference learning with linear function approximation. In *Conference on learning theory*, pages 1691–1692. PMLR, 2018. 6
- [39] Greg Brockman, Vicki Cheung, Ludwig Pettersson, Jonas Schneider, John Schulman, Jie Tang, and Wojciech Zaremba. Openai gym. *arXiv preprint arXiv:1606.01540*, 2016. 8
- [40] Paulo C Heredia and Shaoshuai Mou. Distributed multi-agent reinforcement learning by actor-critic method. *IFAC-PapersOnLine*, 52(20):363–368, 2019. 10
- [41] Paulo Heredia, Hasan Ghadialy, and Shaoshuai Mou. Finite-sample analysis of distributed q-learning for multi-agent networks. In *2020 American Control Conference (ACC)*, pages 3511–3516. IEEE, 2020.
- [42] Kaiqing Zhang, Zhuoran Yang, Han Liu, Tong Zhang, and Tamer Basar. Fully decentralized multi-agent reinforcement learning with networked agents. In *International Conference on Machine Learning*, pages 5872–5881. PMLR, 2018. 10